TECTONICS, VOL. 19, NO. 6, PAGES 1056-1064 DECEMBER 2000

On the relationship between surface uplift and gravitational extension

Kurt Stüwe
Department of Geology, University of Graz, Austria

Terence D. Barr[1]
Department of Earth Science, Monash University, Victoria, Australia

Abstract. This paper highlights the relationship between isostatically supported surface elevation and the lateral buoyancy forces of an orogen. The former is a linear function; the latter is a quadratic function of the thickness of the lithosphere. Thus surface elevation and lateral buoyancy forces may have differing evolutions in the development of an orogen. Indeed, during the evolution of collisional orogens the qualitative relationship between these two parameters may reverse, so that only in the early orogenic evolution, topographically high regions exert a net lateral buoyancy force on topographically low regions. Later in the evolution this may change to a counterintuitive scenario in which there is a net lateral buoyancy force from the topographically lower regions toward the topographically higher regions. To illustrate this fact, we use a simple one-dimensional kinematic model for an orogen which undergoes simultaneous thickening due to convergence and erosion at the surface. It can be shown that for reasonable erosion and thickening rates, surface elevation increases through time until a steady state is reached, while the lateral buoyancy force changes from positive to negative, giving rise to the inward collapse of an orogen. In the field this may be recognized as the occurrence of two successive coaxial convergent deformation events. Present-day examples may be the formation of back arc basins where extension in the low-lying hinterland of an Andean-type mountain belt is caused by a gravitational compressive force exerted by the hinterland onto a belt of significantly higher surface elevation but possibly of lower potential energy.

1. Introduction

Akin to the confusion that is manifested in the literature about the differences between uplift and exhumation [e.g., *England and Molnar,* 1990; *Stüwe and Barr,* 1998], surface elevation and extensional forces in an orogen are also often confused, or it is implied that one causes the other. While this confusion is widespread among many field-oriented papers, we acknowledge that it is well understood in the geophysical literature [e.g., *Coblentz et al.*, 1994; *Wdowinsky and Bock*, 1994; *Jones et al.*, 1996, 1998]. Specifically, many papers do not discriminate between the differences in the vertically integrated vertical stresses in the lithosphere (which are the cause of lateral forces) and differences in surface elevation (which are generally considered as the prime cause of lateral forces). This is illustrated in Figure 1 where three examples of lithospheric thickness cartoons are shown with their relative surface elevations and their relative lateral buoyancy forces. Figure 1 corresponds to similar figures drawn in the past by *Dalmayrac and Molnar* [1981] and *Jones et al.* [1998]. In Figure 1a an intuitive situation is sketched in which the lithospheric column with the higher surface elevation exerts a lateral buoyancy force (black arrow between the two columns) onto the column of lower surface elevation. The magnitude of this force is given by the area between the two σ_{zz} versus z curves. However, in Figure 1b a situation is sketched where the difference in surface elevation is the same as in Figure 1a but no horizontal buoyancy force exists between the two columns, while in Figure 1c a situation is sketched where there is no elevation contrast between the two columns but a horizontal force does exist.

This paper serves to clarify this counter intuitive situation and illustrate, through a simple one-dimensional mode, how qualitative changes between the evolution of surface elevation and lateral buoyancy forces may develop during the evolution of convergent orogens. Thus this paper is meant as a "moderator" of the wide spread belief that high topography corresponds directly to high lateral buoyancy forces. We begin with a review of the basic physical principles.

2. Physical Background

The physical foundation of isostatically supported surface elevation and horizontal buoyancy force have

[1]Now at AFEX International, Houston, TX 77024

Paper number 2000TC900017.
0278-7407/00/2000TC900017$12.00

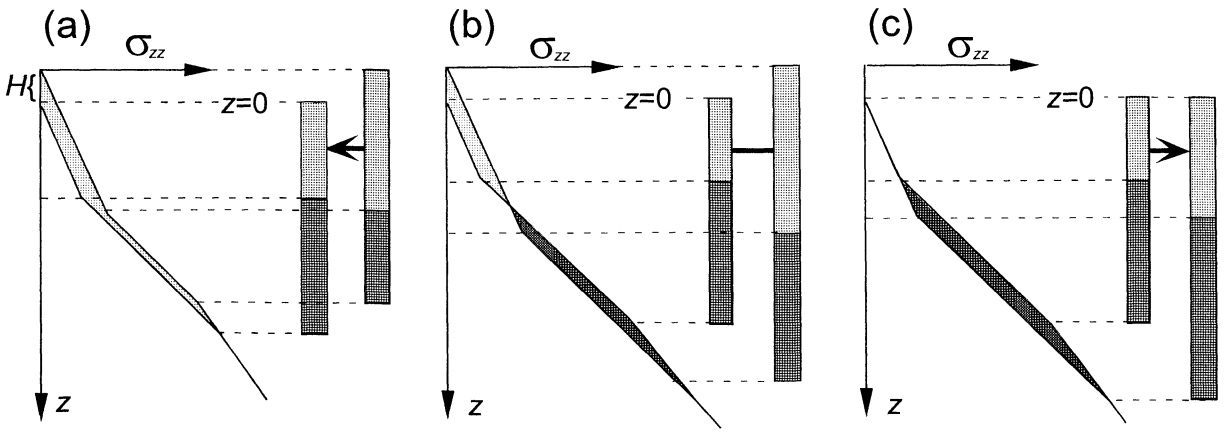

Figure 1. Three possible and qualitatively different relationships between surface elevation and horizontal buoyancy force. In all three examples, two schematic lithospheric columns are drawn on the right (crust is shaded light and mantle lithosphere is shaded dark; see also Figure 2), and a diagram of vertical normal stress (σ_{zz}) against depth (z) is shown on the left. The net force exerted from one column onto the other is given by the area between the two curves on the σ_{zz} versus z diagrams (shaded regions). (a) A reference lithospheric column in comparison with a lithosphere in which the crust is thickened and the mantle part of the lithosphere is thinned. The surface elevation of this column is higher, and there is a lateral force outward from the higher column onto the lower (black arrow between two columns). (b) Two columns that have the same surface elevation contrast as in Figure 1a. However, only in the upper half of the column, a buoyancy force exists from the right to the left column (light shaded area). In the lower part of the column a lateral buoyancy force exists from the left to the right column (dark shaded area). Integrated over the thickness of the lithosphere, no net lateral buoyancy force exists therefore between the columns. (c) Two lithospheric columns with the same isostatically supported surface elevation. However, there is a net lateral buoyancy force from the left column toward the right column.

long been understood (e.g., summary by *Fleitout and Froidvaux* [1982], *Molnar and Lyon-Caen* [1988], *Coblentz et al.* [1994]. The isostatically supported surface elevation of an orogen relative to an undeformed reference lithosphere, H, can be calculated from the difference of the integrals of density from the surface to the isostatic compensation depth z_k between two lithospheric columns M and L, which are to be compared. This integral is equivalent to the difference in the vertical normal stresses σ_{zz} at the depth z_k and may be written as

$$\Delta\sigma = 0 = \sigma_{zz}^{M}|_{z=z_k} - \sigma_{zz}^{L}|_{z=z_K}$$

$$= \int_0^{z_k} \rho^M(z) g dz - \int_0^{z_k} \rho^L(z) g dz. \qquad (1)$$

The superscripts M and L denote the orogen (mountainous region) and the reference lithosphere (lowlands), respectively [for concept of reference lithosphere, see *Le Pichon et al.* 1982]. Here z is depth measured positive downward from the surface of the reference column, $\rho(z)$ is density as a function of z, and g is the gravitational acceleration. Equation (1) can be solved for elevation if it is integrated in parts, for example, as the sum of the integrals between $z = H$ and $z = 0$, between $z = 0$ and $z = z_c$ (the Moho depth), and between $z = z_c$ and $z = z_l$ (the base of the lithosphere, which usually corresponds to z_k) [*Sandiford and Powell*, 1990; *Turcotte and Schubert*, 1982]. According to (1), surface elevation is linear in z. In contrast to (1), the potential energy difference ΔE_p between two lithospheric columns per unit area may be found by the difference between the vertically integrated vertical normal stresses of the two columns. This may be written as

$$\Delta E_p = \int_0^{z_k} \sigma_{zz}^M dz - \int_0^{z_k} \sigma_{zz}^L dz$$

$$= \int_0^z \int_0^{z_k} \rho^M(z) g dz dz - \int_0^z \int_0^{z_k} \rho^L(z) g dz dz. \qquad (2)$$

This integral may be graphically interpreted from the area between two curves plotted on a diagram of σ_{zz} against depth z (Figure 1). ΔE_p may also be interpreted as the horizontal force per meter length of orogen that is exerted from one column onto the other. ΔE_p is therefore often called horizontal buoyancy force F_b. It is this force that gives rise to the gravitational collapse of an orogen. It is defined that $F_b \equiv \Delta E_p$, and we call this force here "lateral force," "net horizontal buoyancy force," or "gravitational force" and keep in

mind that it has the units of force per meter length of orogen. According to (2), the horizontal buoyancy force is quadratic in z.

By comparing the respective linear and quadratic relationships described by (1) and (2) it should be apparent that H and F_b must follow different patterns in time as the thickness of an orogen changes with time. This fact forms the basic premise of this paper, and we will now illustrate their relationship in a simplified time-dependent evolution of a model orogen.

3. Model Description

In order to evaluate the relationships between horizontal buoyance forces and surface elevation in convergent orogens we use a simple one-dimensional model orogen in which lithospheric thickening occurs simultaneously with crustal thinning due to erosion at the surface. Within our model, we describe isostatically supported surface elevation and horizontal buoyancy force both as a function of time using relationships that are well-established in the literature and will not be derived in detail here. In particular, we use integrals of (1) and (2) that were derived using simplified assumptions about the density structure of the lithosphere. Surface elevation is described with the relationship

$$H = \delta z_c(f_c - 1) - \xi z_l(f_l - 1), \tag{3}$$

which stems from integrating (1) [*Sandiford and Powell*, 1990]. The first term of (3) describes the isostatically supported surface elevation due to the density contrast between crust and mantle part of the lithosphere (both of constant density), and the second term describes the surface elevation due to thermal contraction of the lithosphere relative to the asthenosphere. The two terms have opposite sign as they have opposite influence on the surface elevation. Here f_c and f_l are the vertical thickening strains of the crust and the lithosphere; z_c and z_l are the initial thickness of the crust and lithosphere; δ is the density contrast between crust and mantle, $\delta = (\rho_m - \rho_c)/\rho_m$; and ξ is the average thermal expansion of the lithospheric column, $\xi = \alpha(T_l - T_s)/2$, where ρ_m and ρ_c are the mantle and crustal densities, respectively, α is the coefficient of thermal expansion, and T_l and T_s are the mantle and surface temperatures, respectively. Details for the derivation of (3) are discussed by *Sandiford and Powell* [1990], *Zhou and Sandiford* [1992], *Zhou and Stüwe* [1994], and *Stüwe and Barr* [1998].

Horizontal buoyancy forces are described by integrating the vertical stresses throughout the lithosphere for the same density structure for which (3) was derived:

$$\frac{F_b}{\rho_m g z_c^2} = \frac{\delta(1-\delta)}{2}(f_c^2 - 1) - \frac{\alpha T_l}{6(z_c/z_l)^2} \times \left(f_l^2 - 1 - 3\delta(f_c f_l - 1)\right) + \frac{\alpha^2 T_l^2}{8(z_c/z_l)^2}(1 - f_l^2) \tag{4}$$

[*Turcotte*, 1983; *Sandiford and Powell*, 1990]. Both (3) and (4) are plotted in Figure 2 as a function of thickening strain of the crust f_c and thickening strain of the lithosphere f_l. As explained in section 2, the horizontal buoyancy contours (solid lines) are curved on Figure 2 and the elevation contours (dashed lines) are straight lines.

In order to evaluate how surface elevation, horizontal buoyancy force, and the relative relationship between the two may change through time we use the simple one-dimensional kinematic model of *Stüwe and Barr* [1998], which describes the thickness evolution of a convergent orogen during simultaneous lithospheric thickening due to convergence and crustal thinning due to erosion at the surface. Within this model we assume homogeneous constant thickening of the lithosphere at constant strain rate, and we assume that the erosion rate at the surface v_{er} is proportional to surface elevation: $v_{er} = H/E$. While we are aware of the limitations of this assumption (e.g., in the case of an elevated plateau), this model is the closest possible approximation to reality in a one-dimensional model. The erosion constant E defines the proportionality between H and v_{er} and has the units of time. With these assumptions the surface elevation as a function of time can be described by

$$H = \frac{\dot{\epsilon} A}{\dot{\epsilon} - B/E}\left(\mathrm{e}^{t(\dot{\epsilon} - B/E)} - 1\right) \tag{5}$$

and trajectories of individual rocks through depth and time may be described by

$$z = z_i \mathrm{e}^{\dot{\epsilon} t} + \frac{A}{B}\left(1 - \mathrm{e}^{\dot{\epsilon} t}\right) + H\left(\frac{1-B}{B}\right) \tag{6}$$

[*Stüwe and Barr*, 1998]. In (5) and (6), A and B are constants summarizing the initial density structure: $A = \delta z_c - \xi z_l$ and $B = \delta - \xi$. The term $\dot{\epsilon}$ is the thickening strain rate, which is assumed to be constant, and t is time. Here z_i is the initial depth of a chosen rock in the reference column. Using the two values $z_i = z_c$ and $z_i = z_l$ in (6), the time-dependent evolution of crustal and lithospheric thickness can be calculated for a simple but realistic orogenic scenario. These thicknesses can be substituted into (4) to obtain the lateral buoyancy force as a function of time by using

$$f_c(t) = \frac{z_{(z_i = z_c)}(t)}{z_c}, \qquad f_l(t) = \frac{z_{(z_i = z_l)}(t)}{z_l}. \tag{7}$$

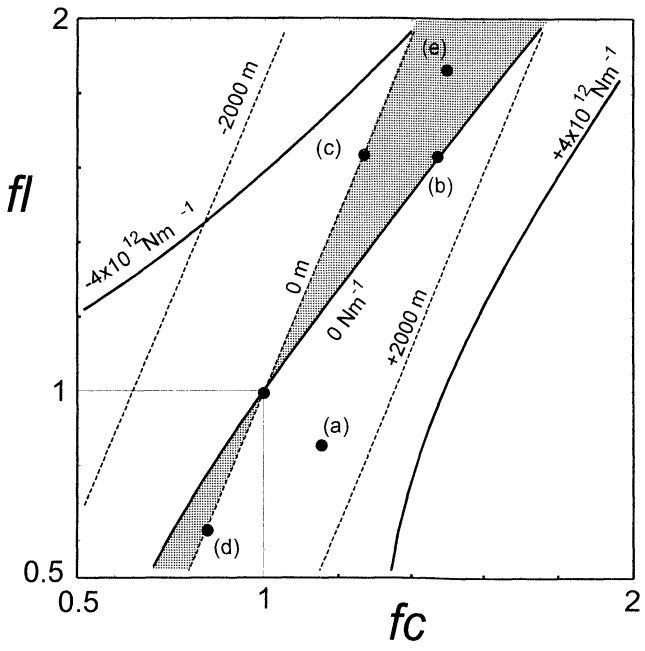

Figure 2. Crustal thickening strain f_c plotted against lithospheric thickening strain f_l and contoured for surface elevation (thin dashed lines are calculated with (3)) and for horizontal buoyancy force (thick curved lines are calculated with (2)). The point marked by the thin lines at $f_c = f_l = 1$ is the reference lithosphere with no thickening strain. In the area below this point the lithosphere is thinner than normal. In the region to the left of this point the crust is thinner than normal. Labeled dots a-c correspond to the thickening geometries shown in Figures 1a-1c (note that a and b have the same surface elevation). Point d shows a location, where the surface is not elevated (like at c) but suffers an opposite horizontal force to c. In the shaded area (e.g., point e) a terrain with lower surface elevation exerts a net lateral buoyancy force onto the area of higher surface elevation.

Thus we have now simple descriptions of both the evolution of surface uplift, (5), and of lateral buoyancy force, (4), as a function of time, and the relationshiop between the two can be easily compared.

4. Model Results

For our calculations, we assumed the following standard values for the physical parameters: $\rho_m = 3200$ kg m^{-3}, $\rho_c = 2700$ kg m^{-3}, $T_l = 1280$°C , $T_s = 0$ °C , $z_c = 35$ km, $z_l = 120$ km, and $\alpha = 3 \times 10^{-5}$ °C $^{-1}$. A strain rate of $\dot{\epsilon} = 10^{-15}$ s^{-1} is assumed. With these parameters the constants in (5) and (6) are $A = 3164$ m and B=0.1371. The erosion parameter E is assumed to have the values $E = 2B/\dot{\epsilon}$, $E = B/\dot{\epsilon}$, $E = B/(2\dot{\epsilon})$, and $E = B/(4\dot{\epsilon})$, which correspond to erosion rates of $v_{er} = H/2.17$ m.y., $v_{er} = H/4.3$ m.y., $v_{er} = H/8.7$ m.y., and $v_{er} = H/17.4$ m.y. This covers a range of geologically realistic erosion rates. The use of full multiples of $B/\dot{\epsilon}$ helps significantly to simplify and understand (5). These parameters differ from those used by *Stüwe and Barr* [1998] only in the value of z_l (which is here 120 km and therefore a bit more realistic than the 100 km assumed by those authors) and the value for strain rate. However, it is noted that in (5) and (6), strain rate and time are directly proportional, so that changing the strain rate by a given factor changes the time in all calculations by the inverse of this factor. All calculations can therefore easily be scaled for time.

Figure 3a shows the development of surface elevation in comparison with the development of horizontal buoyancy force (Figure 3b) as described by (4) and (5). The surface elevation is calculated for an erosion rate of $v_{er} = 2H\dot{\epsilon}/B$ [see *Stüwe and Barr*, 1998, Figure 3a]. The horizontal buoyancy force was calculated after substituting f_c and f_l from (7) in (4), and it is shown for all four different erosion rates listed above. However, only curves with erosion rates faster than $v_{er} > H\dot{\epsilon}/B$ (this is $E < B/\dot{\epsilon}$) are geologically meaningful [*Stüwe and Barr*, 1998]. Thus we focus below only on the lower three curves on Figure 3. Comparison of Figures 3a and 3b shows an extremely interesting result: It may be seen that the horizontal buoyancy force changes from positive values ("outward" from the orogen) to negative values ("inward", toward the orogen) during a continuous increase in surface elevation. This transition occurs well before the steady state surface elevation is reached and is characteristic of all erosion rates. This feature forms the principle result of this paper and the remainder of this paper, will focus on the interpretation of its causes and its geological relevance.

In the remainder of section 4 we interpret the results shown in the first part of the section. Interpretation of Figure 3 is facilitated by reconsidering Figure 2. Figure 2 shows contours for F_b as well as for H as a function of both thickening strain of the crust f_c and thickening strain of the lithosphere f_l. To the right of the $H = 0$ contour, surface elevation is positive, and to the left, surface elevation is negative. Correspondingly, to the right of the $F_b = 0$ contour, the horizontal buoyancy force is positive, and to the left, it is negative. Thus, in the region between the $H = 0$ and the $F_b = 0$ contours, there is a compressive horizontal buoyancy force acting from a topographically low region onto a topographically high region (shaded region).

In a similar way, $f_c - f_l$ trajectories that move away from the $H = 0$ contour lead to larger values of surface elevations (positive or negative), while $f_c - f_l$ trajectories that move away from the $F_b = 0$ contour lead to larger magnitude (positive or negative) values of the horizontal buoyancy forces and vice versa. Thus three types of lithospheric thickening paths are conceivable on Figure 2. First, there are paths that have a shallower slope than both the F_b and the H contours (the

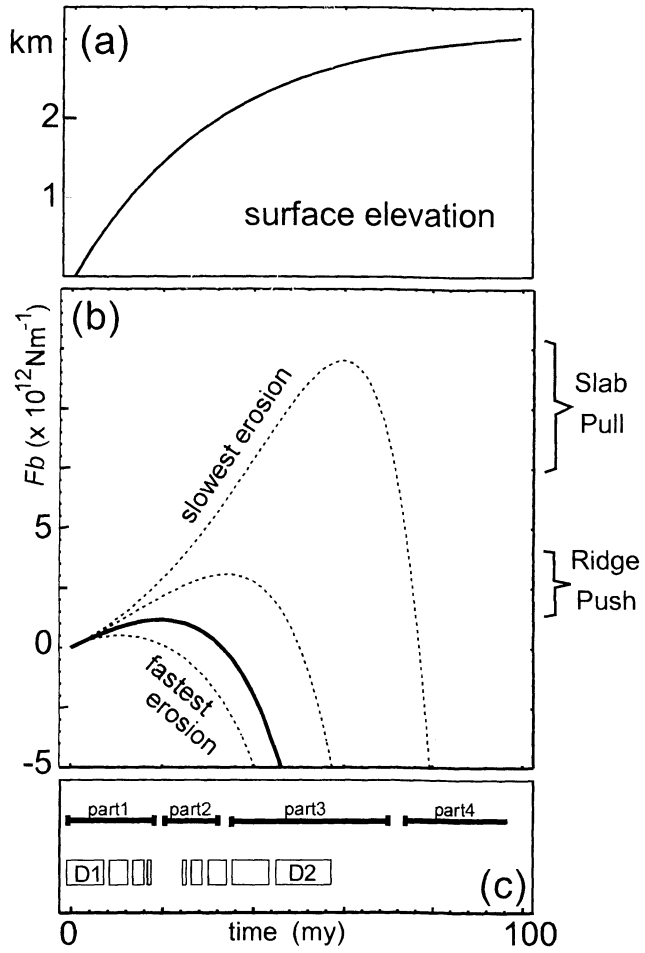

Figure 3. Time-dependent evolution of (a) surface elevation and (b) horizonal buoyancy force within the model assumptions discussed here. Figure 3 is calculated with (4) and (5). F_b evolutions are shown for four different surface erosion rates discussed in the text. The thick line corresponds to the curve shown in Figure 3a. The approximate magnitude of ridge push and slab pull forces are shown for reference. For Figure 3 it was assumed that z_l=100 km. (c) Plot showing the evolution shown in Figures 3a and 3b can be divided into four parts that will be discussed in detail on Figure 4b. Figure 3c also shows the timing of two inferred convergent deformation phases D_1 and D_2; see section 5.

crustal thickness given by f_c increases faster than the lithospheric thickness given by f_l). For such paths, F_b and H both increase in an orogen. Second, there are paths that have a steeper slope than both the F_b and the H contours (f_l increases faster than f_c). For such paths, F_b and H both decrease in an orogen. Third, there are paths with an intermediate slope between the F_b and the H contours (f_l increases only slightly faster than f_c). For such paths, F_b decreases, but the surface elevation increases.

Understanding this, it is now easy to interpret the evolution shown in Figure 3 with the aid of Figure 4: During the initial thickening both crust and mantle part of the lithosphere are thickened leading to surface uplift and an increasing horizontal buoyancy force outwards from the orogen. As surface elevation increases, the erosion rate also increases. Thus the increasingly rapid erosion from above prevents the crust from thickening at the same rate as the mantle part of the lithosphere (which thickens while being unaffected by erosion). Thus the negative buoyancy contribution of the mantle lithosphere will eventually win over the positive buoyancy force contribution of the crust. This is illustrated on Figure 4a, where the thickening strain of crust and lithosphere are both plotted as a function of time for the geologically relevant erosion rates from Figure 3. It may be seen that the temporal evolution of lithospheric thickness is much less sensitive to the erosion rate at the surface than the crustal thickness.

Figure 4b shows one example of an $f_c - f_l$ evolution during simultaneous thickening and erosion at the surface. The diagram is similar to Figure 2 and may be read in direct comparison with Figure 3b. It may be seen that the evolution may be divided into four parts. Initially, surface elevation and horizontal buoyancy force both increase (part 1 on Figure 4b). As elevation increases, the erosion rate increases as well, and the rate of surface uplift decreases (part 2 on Figure 4b). The mantle part of the lithosphere thickens rapidly relative to the crust, so that the orogenic path on Figure 4b becomes curved until the horizontal buoyancy force contours are crossed toward the left. The horizontal force decreases and crosses over to negative values (part 3 on Figure 4b). Only in the final stage the steady state surface elevation is reached, while the inward collapse of the orogen proceeds (part 4 on Figure 4b). Parts 3 and 4 on Fig. 4b correspond to the scenario sketched qualitatively in the cartoon on Figure 1b, where the thickness of the mantle lithosphere of the right-hand column has become so large that the dark shaded region on the σ_{zz} versus z diagram outweighs the light shaded area. Thus, integrated over the thickness of the whole lithosphere, there is a net lateral buoyancy force exerted from the topographically lower region onto the topographically higher region. Clearly, these evolutions are only in part geologically relevant. This will be discussed in section 5.

5. Discussion

Section 1-4 have shown an extremely interesting result, namely, that the lateral buoyancy force of a simple collisional orogen may qualitatively change from outwards from the orogen to inward toward the orogen even though the surface elevation continues to increase at all times. However, before discussing the geological relevance of this result it is important to emphasize the limitations of the model presented here.

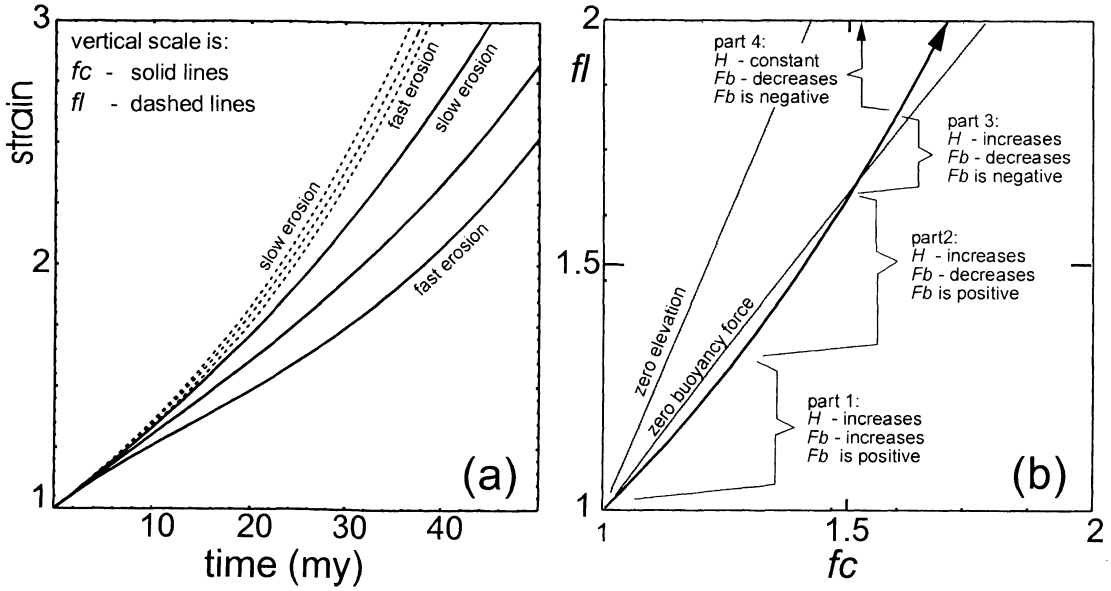

Figure 4. (a) The evolution of f_c (thick lines) and f_l (thin dashed lines) from Figure 3 for the faster three erosion rates. It may be seen that the rate crustal thickening is much slower than lithospheric thickening. (b) The evolution of the lithosphere from Figure 3 shown on an $f_c - f_l$ diagram for medium erosion rates of $v_{er} = 2H\dot{\epsilon}/B$. The evolution may be divided into four parts that can also be identified on Figure 2 and that are labeled on Figure 3c.

5.1. Limits of Geological Relevance

5.1.1. Parameter ranges. Of the parameters used for the calculations the largest uncertainty is about the initial thickness of the lithosphere at the onset of an orogenic evolution. For example, in some stable cratons the thermally stabilized lithosphere is some 200 km thick, while in many other stable continental regions the lithosphere is only ≈120 km thick. In order to explore the influence of such different thicknesses we show in Figure 5 the shaded region of Figure 2 as a function of $\psi = z_c/z_l$: the initial ratio of crustal thickness to lithospheric thickness. It may be seen that the region in which topographic lows exert a net horizontal buoyancy force onto topographic highs increases with thicker intial lithospheres (smaller ψ). In particular, for $\psi < 0.25$, even homogeneous lithospheric thickening will lead to the counter intuitive situation discussed above, and it is therefore not unreasonable to expect some field examples where this can be observed.

5.1.2. One dimensionality. The model discussed above is one-dimensional and does not consider the two- or even three-dimensional complications in the stress or strain field occurring in most real orogens [e.g., *Platt*, 1993]. As such, the model is not directly applicable to many real orogens, which are, for example, often not in isostatic equilibrium. Rather, the model presented here should be seen as a cartoon illustrating some simple, but often confused, phsyical principles. Its merits lie in the clarity, which is a mandatory requirement to understand the basic principles highlighted herein. We believe that any more complicated (and possibly more realistic and applicable) model would obscure the physical processes emphasized here and would therefore do a disservice to the fundamental aim of this paper.

A more serious model constraint than the one dimensonality assumption is the assumption that horizontal buoyancy force is derived by vertically integrating the lateral stresses. Thus we do not consider vertical changes in the lateral force. For example, on Figure 1, there is always a horizontal buoyancy force exerted from the topographic high toward the topographic low in the upper part of the column. Only in the lower part of the column this relationship reverses in Figure 1b, so that the integrated net force from one column onto the other is zero. In real orogens, such a scenario may lead to the development of shear zones near the depth where the relative magnitude of the vertical stresses reverses between the two columns. The model discussed here may therefore only be relevant to mechanically strong lithospheres, where the arising shear forces are hindered to cause shear strains at depth and a vertical integration of lateral forces is allowed (for a similar discussion, see *Avouac and Burov* [1996]). It may be possible to infer reversals in the direction of lateral forces by interpreting the depth dependence of fault plane solutions.

5.1.3. Temporal and magnitude limitations. Figure 4a shows that, for the assumed strain rate – the lithosphere exceeds a geologically meaningful thickening strain after ≈30 m.y. (it reaches double thickness after ≈20 m.y.). This is a function of the assumed constant strain rate and implies that interpretation of

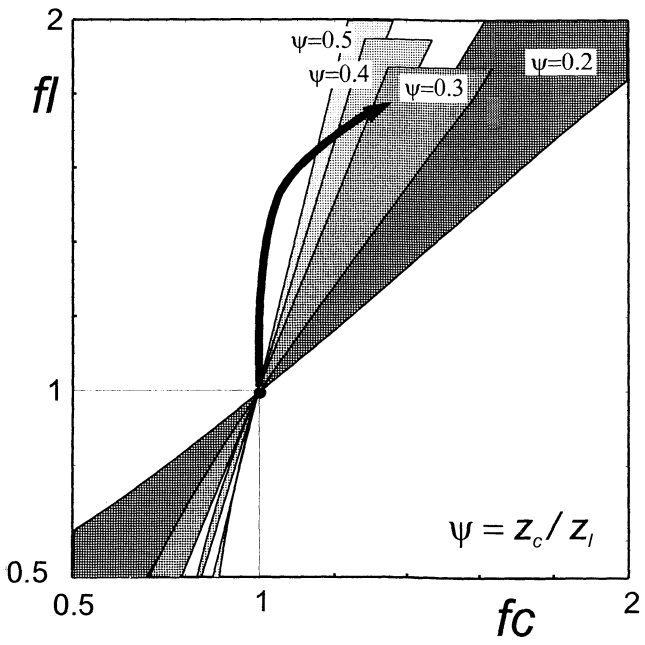

Figure 5. An $f_c - f_l$ diagram showing the parameter space in which there is a net horizontal buoyancy force from the topographically lower regions onto topographically higher regions explored for a range of initial ratios of z_c to z_l. It may be seen that, in particular for thick initial lithospheres ($\psi = 0.2$), this region covers geologically relevant thicknesses for crust and mantle lithosphere in orogens. The thick path is discussed in the text.

Figure 3 beyond 30 m.y. is not meaningful. However, it may be seen on Figures 3 and 4b that the reversal of F_b from positive to negative occurs already well before this. Moreover, the curves on Figure 3 are self-similar, so that curves for any erosion rate and strain rate will show this feature. Thus the effect of a qualitative lateral buoyancy force reversal may occur at all times in the thickness evolution of an orogen. Figure 3 also shows that the absolute magnitude of the lateral forces may be small compared with the tectonic driving forces, for example, ridge push or slab pull. However, in view of the fact that lateral extension can occur in directions orthogonal to the tectonic convergence and the fact that orogenic collapse often occurs after the tectonic driving forces have waned, the buoyancy forces can be considered independent of the tectonic driving force. Moreover, the principle occurrence of the reversal of the lateral force will always have an influence on the orogenic force balance (see below) and therefore may ultimately imply surges in the strain rate evolution of an orogen [see also *Avouac and Burov*, 1996].

5.2. Geological Examples and Field Evidence

Figure 3b shows that the horizontal buoyancy force in orogens may first increase and later decrease and eventually change from positive (outward from the orogen) values to negative values (toward the orogen). The implication of this may be understood in terms of the effective driving force F_{eff} that is applied to a convergent orogen. This effective driving force may be viewed as the difference between the tectonic driving force F_d and F_b:

$$F_{\text{eff}} = F_d - F_b \tag{8}$$

[e.g., *Sonder and England*, 1986; *Zhou and Sandiford*, 1992]. In comparison with Figure 3b, this equation states that the effective driving force has a minimum during a continuous evolution of convergence. In the early evolution of an orogen, F_b is small, and the effective driving force is governed by the onset of convergence. Thereafter, F_{eff} decreases as F_b increases. After F_b has gone past its maximum the effective driving force increases again. In the field this occurrence of a minimum in F_{eff} shortly after the onset of an orogenic evolution may be reflected in the development of two colinear deformation phases (labeled as D_1 and D_2 in Figure 3c). The occurrence of two colinear early defomation phases is indeed common to many mountain belts, for example, eastern Antarctica [*Hand et al.*, 1994], Namibia [*Dürr and Dingeldey*, 1996], central Australia [*Goscombe*, 1991] or the Adelaide Fold Belt [*Oliver and Zakowski*, 1995]. However, in view of the kinematic boundary conditions of the model discussed here, we will not discuss this potential example further. Any valued discussion of this observation must be performed on hand of a similar model subjected to stress boundary conditions.

Figures 2 and 5 show that topographic lows may exert net horizontal buoyancy forces onto topographic highs in two different areas of parameter space: first, in extensional environments where $f_c < 1$ and $f_l < 1$ (this is the part of the "bow tie" in the bottom left of Figures 2 and 5) and second, in collisional environments where $f_c > 1$ and $f_l > 1$ ("bow tie" in the top right quadrant of Figures 2 and 5). There examples are particularly likely in regions where $f_c < f_l$, that is, where the mantle part of the lithosphere is even more thickened than the crust. While this parameter space may be reached in a range of orogenic environments, we believe that this setting may be exemplified by subduction zone environments where the process discussed here may contribute to the development of fore arc or back arc basins.

In subduction zones, entire slabs of oceanic lithosphere are emplaced underneath the margins of continental lithosphere. Because the thickness of the oceanic crust is negligible and that of the oceanic mantle lithosphere is comparable to that of the continental mantle lithosphere, this process leads to an immediate doubling of the mantle lithosphere underneath the continent, while the total crustal thickness remains comparably unaffected. Simultaneousy with or subsequent to this process, convergence or underplating will lead to

some thickening of the crust. This thickening evolution is illustrated by the thick path of Figure 5. This path enters the shaded area where topographically lower regions exert a net lateral buoyancy force onto topogaphically higher regions. Thus it is possible that Andean-type mountain belts with significant surface elevation have, despite their high topography, a lower potential energy than their surroundings, at least during some stages of their evolution. Albeit the fact that Andean-type mountain belts may not be in isostatic equilibrium, this may cause gravitational forces to act from the hinterland or foreland onto the mountain belt. These forces would act in addition to the overall far-field driving forces. This then may result in extensional collapse of the hinterland or foreland towards the mountain belt, forming back arc or forearc basins. It is therefore possible that the formation of backarc or forearc basins is unrelated to the overall kinematics of the subduction zone and also need not be related to processes in the mantle wedge and other processes that have been made responsible for backarc basin extension (e.g., see summary by *Allen and Allen* [1990]).

One example where this process may be of relevance is the central Andes. Figure 6 shows a schematic cross section through a subduction zone as it is now a well-accepted model for such environments [e.g., *Turcotte and Schubert*, 1982] and which is consistent with recent detailed work by a major German geophysical Andean transsect (e.g., *Graeber and Asch*, [1999]; see also http://www.fu-berlin.de/sfb267/). Three important profiles are emphasized on Figure 6. Profile a is the stable hinterland in the far field, where continental crust and mantle part of the lithosphere are of reference thickness. Profile b is in the foreland where the continental crust has a near normal thickness and the mantle part of the lithosphere consists of a sliver of continental mantle lithosphere plus the full oceanic lithosphere. Profile c is in the center of the mountain belt where the crust is overthickened and the mantle part of the lithosphere is overthickened as well. Note that the Moho and the upper surface of the subducting plate diverge between profiles b and c, so that the overthickening of the mantle part of the lithosphere is more rapid than the overthickening of the crust as profile c is approached. This is consistent with the arrow on Figure 5. The thickening geometries of profiles a, b and c are consistent with those required for gravitational forces to arise, which are exerted from topographic lows toward topographic highs. These are indicated by the small white (schematic) arrows underneath profiles a and b.

Profiles b and c are consistent with the geometry of the central Andes at longitudes 69.5°W and 68.5°W [e.g., *Graeber and Asch*, 1999]. There the region corresponding to profile b is characterized by a longitudinal valley between the Coastal Cordillera and the Precordillera, while profile c is consistent with the region of the high topography of the Western Cordillera. We are startled by the idea that this observation may be explained by the model discussed here; that is, the region of the longitudinal valley is characterized by gravitational extension toward the Western Cordillera. One test to this interpretation would be an investigation of the asymmetry of the forearc basin. Standard models appealing to rollback or mantle wedge processes imply a symmetric extension in the forearc or retroarc. The model invoked here implies an asymmetry of the formed basin with the depot center nearest the region of high topography. Although some asymmetric basins developed in the Peruvian Andes [*Dalmayrac and Molnar*, 1981] are unrelated to the regions of interest discussed here, we suggest that our model is potentially testable in the foreland and hinterland of Andean-type mountain belts.

6. Conclusion

Surface elevation and horizontal buoyancy forces are linear and quadratic functions of the density distribu-

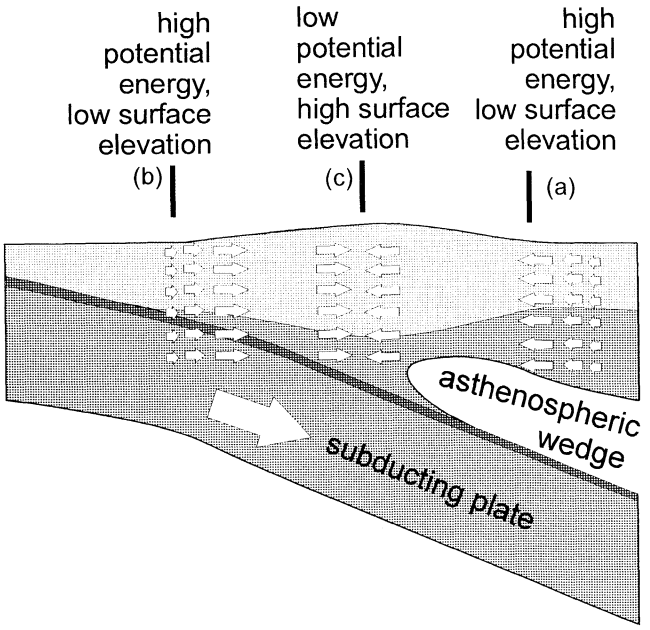

Figure 6. Cartoon showing the geometry of subduction zone environments. The large white arrow in the subducting plate indicates the motion of the subducting slab. The small white arrows indicate the stress field arising from gravitational potential energy differences at the three labeled vertical sections. Light shaded region is continental crust, medium dark shaded region is lithospheric mantle, and dark shaded area is oceanic crust. Note that going from both profiles a and b toward profile c thickening of the mantle part of the lithosphere is greater than thickening of the crust. For details, see text.

tion in the lithosphere, respectively. Thus surface elevation and horizontal force need not correlate directly, and it is dangerous to imply that topographically higher regions always exert a net horizontal buoyancy force onto topographically lower regions. For some realistic thickening geometries of crust and mantle part of the lithosphere, topographically lower regions may exert net lateral buoyany forces onto topographically higher regions.

As a consequence, the relationship between surface uplift and lateral buoyancy force may reverse during a continuous thickness evolution of an orogen. For example, early in the orogenic evolution, surface uplift may be accompanied by an increasing lateral force outward from the elevated region. Later in the same evolution, continuing surface uplift may be accompanied by decreasing or even negative buoyancy forces, giving rise to the gavitational inward collapse of the elevated region. Then, extension in the foreland and accellerated compression in the orogen should be observed.

We believe that this process may be observed in Andean-type mountain belts, where the region of highest topography may have a lower gravitational potential energy than the foreland and hinterland. Thus the formation of forearc or retroarc basins may be related to gravitational collapse of these regions toward the region of significantly higher topography.

Acknowledgments. G. Houseman and H. Fritz are thanked for a series of discussions about the story of this paper. N. Mancktelow and D. Coblentz are thanked for a number of comments on a presubmission version of the manuscript. D. Davis, J. Van Den Driesche, and F. Roure are thanked for their positive comments and compliments during the review stage. M. Sandiford is thanked for introducing us to the $f_c - f_l$ plane and, in fact, for implicitly solving the problem present here many years ago. F. Graeber is thanked for bringing the deep structure of the Andes to our attention and M. Hand for extending our knowledge of the number of terrains with early colinear deformation phases. This study was supported by FWF project P-12846-GEO.

References

Allen, P.A., and J.R. Allen, Basin Analysis. Principles and Applications, 450 pp., Blackwell Sci., Malden, Mass., 1990.

Avouac, J.P., and E.B. Burov, Erosion as a driving mechanism of intracontinental mountain growth, *J. Geophys. Res., 101*, 17,747-17,769, 1996.

Coblentz, D., R.M. Richardson, and M. Sandiford, On the potential energy of the Earth's lithosphere, *Tectonics, 13*, 929-945, 1994.

Dalmayrac, B., and P. Molnar, Parallel thrust and normal faulting in Peru and constraints on the state of stress, *Earth Plant. Sci. Lett., 55*, 473-481, 1981.

Dürr, S., and D.P. Dingeldey, The Kaoko belt (Namibia): Part of a late Neoproterozoic continental-scale strike slip system, *Geology, 24*, 503-506, 1996.

England, P.C., and P. Molnar, Surface uplift, uplift of rocks and exhumation of rocks, *Geology, 18*, 1173-1177, 1990.

Fleitout, L., and C. Froidvaux, Tectonics and topography for a lithosphere containing density heterogeneities, *Tectonics, 1*, 21-57, 1982.

Goscombe, B., Intense non-coaxial shear and the development of mega scale sheath folds in the Arunta Block, central Australia, *J. Struct. Geol., 13*, 299-318, 1991.

Graeber, F.M., and G. Asch, Three dimensional model of P wave velocity and P-to-S velocity ratio in the southern central Andes by simultaneous inversion of local earthquake data, *J. Geophys. Res., 104*, 20,237-20,256, 1999.

Hand, M., I. Scrimgeour, R. Powell, K. Stüwe, and C.J.L. Wilson, Metapelitic granulites from Jetty Peninsula, east Antarctica: formation during a single event or by poly metamorphism?, *J. Metamorph. Geol., 12*, 557-573, 1994.

Jones, C.H., L.J. Sonder, and J.R. Unruh, Lithospheric gravitational potential energy and past orogenesis: implications for conditions of intial Basin and Range and Laramide deformation, *Geology, 26*, 639-642, 1998.

Jones, C.H., J. Unruh, and L.J. Sonder, The role of gravitational potential energy in active deformation in the south western US, *Nature, 381*, 37-41, 1996.

Le Pichon, X., J. Angelier, and J.C. Sibuet, Plate boundaries and extensional tectonics, *Tectonophysics, 81*, 239-256, 1982

Molnar, P., and H. Lyon-Caen, Some simple physical aspects of the support, structure and evolution of mountain belts, *Spec. Pap. Geol. Soc. Am., 218*, 179-207, 1988.

Oliver, N.H.S., and S. Zakowski, Timing and geometry of deformation and low-pressure metamorphism in the eastern Mount Lofty Ranges: The possible role of extension, *Aust. J. Earth Sci., 42*, 501-507, 1995.

Platt, J.P., Mechanics of oblique convergence, *J. Geophys. Res., 98*, 16,239-16,256, 1993.

Sandiford, M., and R. Powell, Some isostatic and thermal consequences of the vertical strain geometry in convergent orogens, *Earth Planet. Sci. Let., 98*, 154-165, 1990.

Sonder, L.J., and P. England, 1986, Vertical averages of rheology of the continental lithosphere: Relation to thin sheet-parameters, *Earth Planet Sci. Lett., 77*, 81-90, 1986.

Stüwe, K., and T. Barr, On uplift and exhumation during convergence, *Tectonics, 17*, 80-88, 1998.

Turcotte, D.L., Mechanisms of crustal deformation, *J. Geol. Soc. London, 140*, 701-724, 1983.

Turcotte, D.L., and G. Schubert, Geodynamics: Applications of Continuum Physics to Geological Problems, 450 pp., John Wiley, New York, 1982.

Wdowinsky, S., and Y. Bock, The evolution of deformation and topography of high elevated plateaus, 1, Model, numerical analysis, and general results, *J. Geophys. Res., 99*, 7103-7119, 1994.

Zhou, S., and M. Sandiford, On the stability of isostatically compensated mountain belts, *J. Geophys. Res., 97*, 14,207-14,221, 1992.

Zhou, S., and K. Stüwe, Modeling of dynamic uplift, denudation rates and thermomechanical consequences of erosion in isostatically compensated mountain belts, *J. Geophys. Res., 99*, 13923-13939, 1994.

K. Stüwe, Department of Geology and Palaeontology, University of Graz, Heinrichstrasse 26, A-8010 Graz, Austria. (e-mail: kurt.stuewe@kfunigraz.ac.at)

T. D. Barr, Department of Earth Science, Monash University, Clayton, Victoria 3168, Australia. (e-mail: terence@earth.monash.edu.au)

(received February 16, 2000;
accepted May 23, 2000.)